

# Comparison between magnetic resonance imaging and fetopathology in the evaluation of fetal posterior fossa non-cystic abnormalities

B. TILEA\*, A. L. DELEZOIDE†, S. KHUNG-SAVATOVSKI†, F. GUIMIOT†, E. VUILLARD‡, J. F. OURY‡ and C. GAREL§

\*Service d'Imagerie Pédiatrique, †Service de Biologie du Développement and ‡Service de Gynécologie Obstétrique, Hôpital Robert Debré, AP-HP, Paris VII Denis Diderot University and §Service de Radiologie, Hôpital d'Enfants Armand-Trousseau, AP-HP, Paris, France

**KEYWORDS:** brain stem; cerebellum; fetus; magnetic resonance; pathology; posterior fossa; prenatal diagnosis

## ABSTRACT

**Objectives** To compare magnetic resonance imaging (MRI) and fetopathological findings in the evaluation of non-cystic fetal posterior fossa anomalies and to describe associated abnormalities.

**Methods** This was a prospective study from 2000 to 2005 of fetuses identified on ultrasound as having sonographic suspicion of posterior fossa malformation. All underwent a thorough MRI examination of the fetal brain, after which we classified each fetus as presenting one of the following pathologies: vermian hypoplasia or agenesis, cerebellar and/or brain stem hypoplasia, destructive or dysplastic lesions. All of the pregnancies were then terminated, after which the whole fetus underwent fetopathological examination. We compared the findings from MRI and fetopathological examinations and recorded the associated cerebral and extracerebral abnormalities.

**Results** Twenty-five fetuses were included. MRI was performed at a mean gestational age of 31 weeks, and fetopathological examination at 33 weeks. In 12 cases we observed vermian hypoplasia, six had partial vermian agenesis, 11 had cerebellar hemisphere hypoplasia, seven had brain stem hypoplasia, four had destructive lesions and six had dysplastic lesions. The two techniques were similar in their performance with respect to the detection of vermian agenesis, brain stem hypoplasia and destructive lesions. There were four false-positive results of MRI for vermian hypoplasia and a poor agreement regarding cerebellar hemisphere hypoplasia. No dysplastic lesions were diagnosed by MRI. None of the posterior

fossa malformations was isolated and many cerebral and extracerebral abnormalities were found.

**Conclusion** A systematic analysis of the posterior fossa in fetal MRI makes it possible to diagnose accurately most posterior fossa malformations. These malformations never occurred in isolation in our study. Copyright © 2007 ISUOG. Published by John Wiley & Sons, Ltd.

## INTRODUCTION

The prenatal diagnosis of fetal posterior fossa abnormalities is challenging; not only is it commonly accepted that this diagnosis is difficult, but the consequences are grave, because most cases have a poor prognosis and lead to a proposal of termination of pregnancy. Some classifications of cerebral malformations, particularly cerebellar ones, have been proposed<sup>1,2</sup>, but these are not always appropriate in fetal imaging. A new classification of abnormalities of the posterior fossa was published recently<sup>3</sup>, based on terminology adequate for differentiating entities such as agenesis, hypoplasia and atrophy. Recent advances in fetal imaging, and particularly in fetal magnetic resonance imaging (MRI), have allowed a more accurate anatomical approach to the structures of the posterior fossa. The degree of agreement between prenatal imaging and pathological findings has been studied with respect to ischemic lesions<sup>4</sup> and fetal brain abnormalities<sup>5</sup>. Pre- and postnatal MRI findings have also been compared in the diagnosis of isolated inferior vermian hypoplasia<sup>6</sup>. So far, no study has focused on the degree of agreement between fetal MRI and fetopathology regarding the evaluation of abnormalities of the cerebellum and brain stem. Therefore, the aim

Correspondence to: Dr C. Garel, Service de Radiologie, Hôpital d'Enfants Armand-Trousseau, 26-28 Avenue du Docteur Arnold Netter, 75571 Paris Cedex 12, France (e-mail: catherine.garel@trs.aphp.fr)

Accepted: 7 February 2007

of our study was to compare the prenatal MRI diagnosis of posterior fossa abnormalities with subsequent pathological findings.

## METHODS

This was a prospective study conducted between January 2000 and December 2005 on a cohort of fetuses identified on ultrasound as having suspicion of posterior fossa malformations. These fetuses then underwent MRI and the study group included all in which MRI detected anomalies of the brain stem and/or cerebellum and for which termination of pregnancy was elected after informed parental consent. A complete fetopathological examination was performed in all cases. Fetuses with evidence of myelomeningocele and Chiari II malformation were excluded. The gestational age was determined by early first-trimester ultrasound examination and was confirmed by fetopathological examination.

### Sonography

In this study, sonography was used as a method of detection of the posterior fossa abnormalities, and our aim was not to evaluate the accuracy of ultrasound in their diagnosis. Therefore, while a transverse slice at the level of the cerebellar hemispheres was acquired systematically, a midline sagittal slice and a coronal slice of the posterior fossa were not. The transvaginal approach was not used systematically.

For all fetuses, the following data were recorded: the gestational age at which ultrasound revealed the anomaly, and/or the gestational age at which ultrasound was performed prior to detection with MRI; the transverse cerebellar diameter (TCD); the biometry of the cisterna magna (this was considered enlarged when its midsagittal depth, measured on a transverse slice at the level of the cerebellar hemispheres from the inner table of the occiput to the posterior aspect of the cerebellum, was  $> 10$  mm<sup>7</sup>); possible cerebellar hemisphere anomalies or cystic lesions of the posterior fossa; the association with other supratentorial or extracerebral anomalies.

### Fetal MRI

MRI was performed on a 1.5-T Unit (Integra, Philips, Best, The Netherlands), 30–40 min after fetal sedation achieved by maternal oral administration of 1 mg flunitrazepam. Examination of the fetal brain was performed using a phased-array abdominal coil, T1-weighted spin echo (SE), spectral presaturation inversion recovery (SPIR) and fat-saturated sequences (697/14/2;  $\alpha = 90^\circ$ ;  $256 \times 256$ ; field of view (FOV), 32 cm; section thickness, 4 mm; acquisition time, 2 min 56 s; 15 sections) in two planes of space, and T2-weighted single-shot turbo SE imaging (24 617/100/1;  $\alpha = 90^\circ$ ;  $256 \times 256$ ; FOV, 280 cm; section thickness, 3 mm; acquisition time, 24 s) was acquired in three orthogonal planes. The gestational age at which MRI was performed was recorded.

In all cases, a thorough analysis of the posterior fossa was conducted, which included the following parameters.

- Biometric parameters. These included the TCD, anteroposterior diameter, height and surface of the vermis. They were measured according to a previously published method and the data were compared with the normal published data as a function of the gestational age<sup>8,9</sup>.
- Vermis. The presence or absence of the primary fissure and the possible presence of another fissure were reported. The posterior/anterior lobe ratio was evaluated subjectively, and we specified whether it was normal (2 : 1) or decreased, according to recently published fetal MRI landmarks<sup>10</sup>.
- Cerebellar hemispheres. The size of each hemisphere was considered normal when its anteroposterior diameter (on an axial slice) was half the TCD. Moreover, we specified whether cerebellar hemispheres were symmetrical or asymmetrical.
- Morphology of the fourth ventricle. This was considered normal if it had a triangular shape and was completely covered by the vermis. It was noted as being open, or uncovered, when a large communication between the fourth ventricle and the cisterna magna was found.
- Brain stem. This was assessed subjectively, as there are presently no published standards for biometry of the brain stem in fetal MRI. The presence or absence of the bulge of the pons was reported. The biometry of the brain stem was considered decreased if the bulge of the pons was absent and/or if the brain stem had a globally thin appearance (Figure 1).
- Insertion and orientation of the tentorium cerebelli. This was considered normally inserted if the tentorium attachment was facing the inion and the upper muscular insertion of the neck<sup>1</sup>. The orientation of the tentorium was assessed subjectively.
- Cisterna magna. This was measured on an axial slice from the midline posterior aspect of the vermis to the inner margin of the occiput<sup>11</sup>. It was considered enlarged if its measurement was  $> 10$  mm and normal if it was  $\leq 10$  mm.
- Other associated cerebral anomalies were reported if present.

Following this analysis of the anatomical posterior fossa structures, we classified each fetus as presenting one of the following pathologies: agenesis of the vermis, hypoplasia or a destructive lesion. Agenesis of the vermis referred to a complete or partial absence of this structure. In the case of partial agenesis, the remaining part of the vermis was anatomically of normal volume (Figure 2). Hypoplasia of the cerebellum (Figure 3) or brain stem (Figure 1) was defined as a small but complete anatomical structure<sup>3</sup>. A destructive lesion was defined as partial or complete loss of an anatomical structure, with focal decreased biometry and possible evidence of an abnormal signal<sup>12</sup> (Figure 4).

The different MRI criteria leading to these diagnoses are summarized in Table 1.

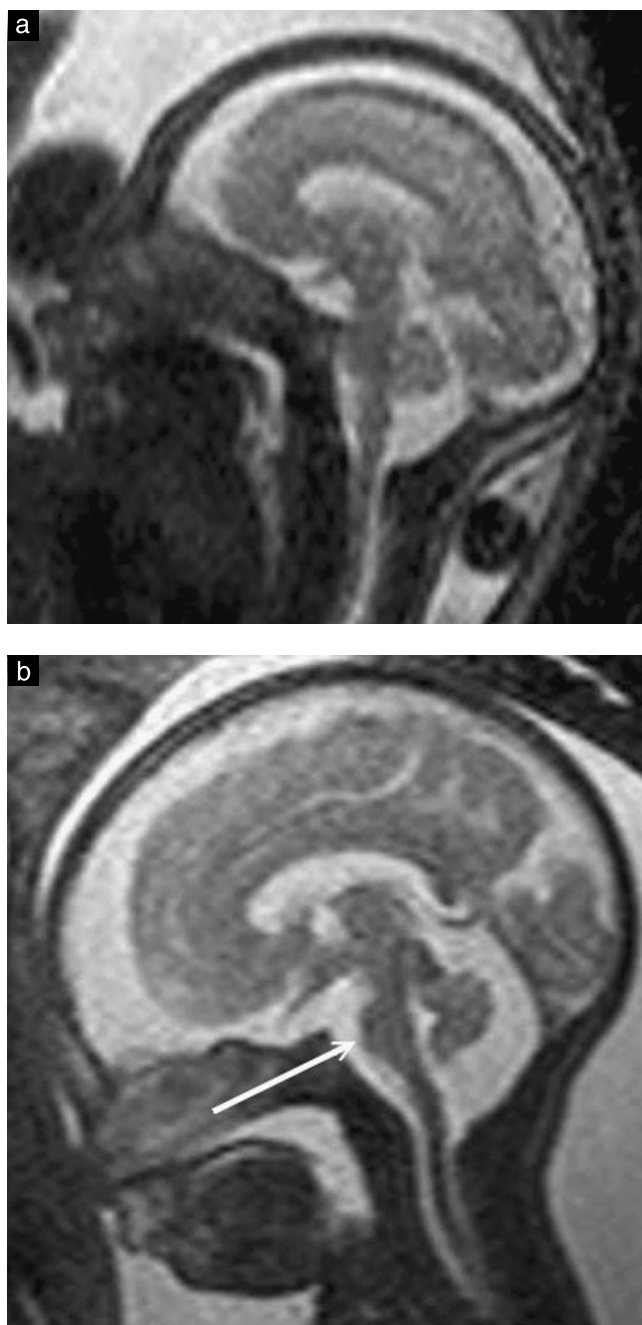


**Figure 1** Magnetic resonance imaging (MRI) of brain stem hypoplasia illustrating two different MRI patterns. (a) Case 2: the brain stem is thin and the bulge of the pons is absent. (b) Case 6: the bulge of the pons is present (arrow) but the brain stem has a globally thin appearance.

**Fetopathological examination**

The gestational age at which termination of pregnancy was performed was recorded. Termination was achieved by feticide followed by induction of labor. Delivery usually occurred within 24 h following feticide, and fetopathological examination was performed within 24 h after delivery, allowing good brain preservation. In all cases, karyotyping was performed, X-rays and photographs of the fetus were acquired and the placenta was examined.

**Table 1** Criteria of the different pathologies detected by magnetic resonance imaging in 25 fetuses with suspected posterior fossa abnormalities

Anatomical structure	Biometric parameters	Vermis	Cerebellar hemispheres	Fourth ventricle	Brain stem (bulge of the pons)	Tentorium cerebelli	Fluid space of the posterior fossa
Hypoplasia Vermis	Decreased	Primary fissure ± secondary fissures, preserved 2/1 ratio	Normal morphology, symmetrical aspect	Normal shape	Normal	Normal position, normal insertion	Enlarged
Cerebellum ± brain stem Agensis Vermis	Decreased	Normal/decreased	Decreased	Normal shape	Normal/decreased	Normal or more vertically inserted	Enlarged
Destructive lesion Vermis and/or cerebellar hemispheres	TCD normal/slightly increased/reduced	Presence or absence of the primary fissure or posterior lobe, non-preserved 2/1 ratio	Abnormally spread or close together	Enlarged, uncovered	Normal	Normal position, normal insertion	Enlarged, abnormal communication between the cisterna magna and the fourth ventricle
	Focal decrease, amputation	Normal/decreased	Normal/decreased	Normal/enlarged	Normal/decreased	Normal	Enlarged

TCD, transcerebellar diameter

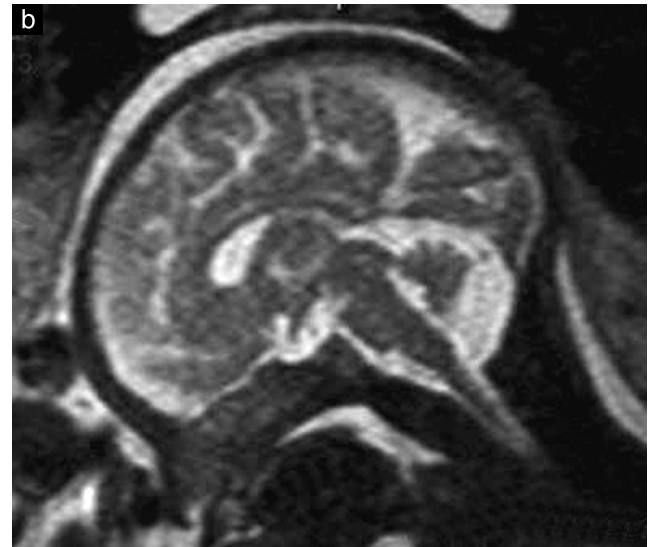
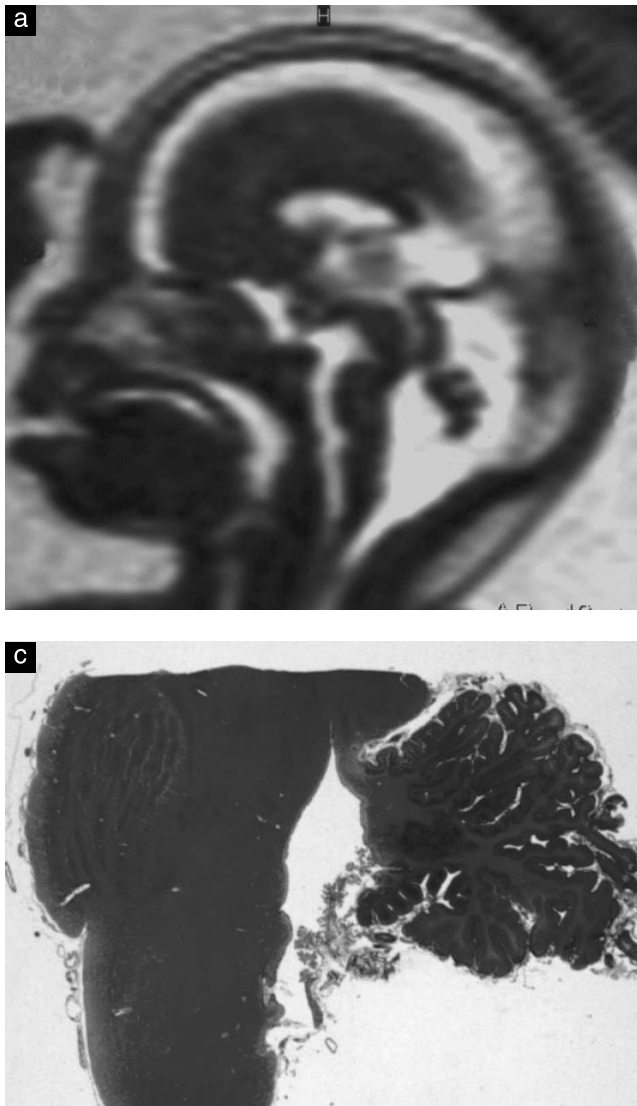


**Figure 2** Magnetic resonance imaging and fetopathology of partial vermian agenesis. (a) Case 12: midline T2-weighted sagittal slice showing enlarged fourth ventricle, decreased vermian biometry, abnormal posterior/anterior lobe ratio and enlarged fluid space of the posterior fossa. These findings are suggestive of posteroinferior vermian agenesis, which was confirmed by fetopathology. (b) Case 20: midline T2-weighted sagittal slice showing abnormally shaped non-triangular fourth ventricle, decreased vermian biometry and enlarged fluid space of the posterior fossa, suggestive of partial vermian agenesis. (c) Case 20: fetopathological examination; midline histological view of the vermian, confirming the posteroinferior vermian agenesis.

The fetopathological analysis included external biometry and examination of the fetus, complete autopsy with dissection and histological examination of the thoracoabdominal organs in order to detect dysmorphic features and extracerebral malformations or lesions. The brain was removed with special attention being paid to the level of insertion of the tentorium cerebelli on the occipital bone and to the internal volume and content (presence of cyst) of the posterior fossa. After the brain was fixated in 4% salted formaldehyde for 2–3 weeks, neuropathological study determined the following parameters:

- Biometric values. The brain weight was recorded. Then, the infratentorial part of the brain including the brain stem and cerebellum was cut just below the inferior colliculi and weighed separately. The maximum TCD was measured. The results were compared with published standards<sup>13–15</sup>. After sagittal section of the infratentorial structures, the height and anteroposterior diameter of the vermian were noted and, because of the absence of anatomical standards, these were compared with MRI normal values<sup>9</sup>.

- Vermian structure. This was analyzed on a sagittal plane. The nine lobules were counted and the vermian was assessed as being complete or incomplete.
- Size and morphology of the cerebellar hemispheres.
- Shape of the fourth ventricle. This was assessed as being normal or open. The presence of a cyst was reported.
- Brain stem. The presence or absence of the bulge of the pons was reported, as well as pyramidal tract and olivae medullae oblongatae relief.

This macroscopic analysis was followed by a detailed histological examination of the brain, including notably the identification of areas of necrosis and hemorrhage, a study of the cortical lamination and a search for migration abnormalities. Histological identification of posterior fossa cyst walls was performed in order to differentiate pure arachnoid cysts from dilated fourth ventricles.

Following this analysis of the posterior fossa structures, we concluded that each fetus presented one of the following pathologies: partial or total agenesis of the vermian; vermian hypoplasia; cerebellar hypoplasia; destructive lesion; dysplasia. Partial or total agenesis of the vermian referred to cases with complete or partial absence of the structure. Vermian hypoplasia was diagnosed when the anatomical structure was complete but small (height and anteroposterior diameters < 10<sup>th</sup> percentile for gestational age). Cerebellar hypoplasia was diagnosed if TCD and infratentorial parts of the brain weighed

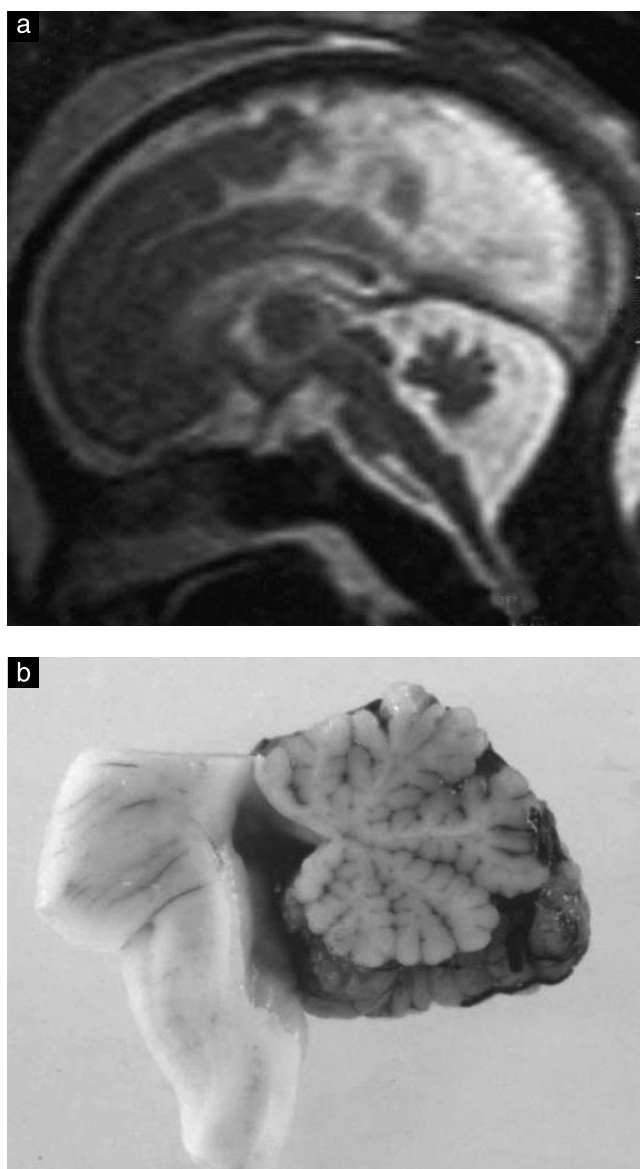


**Figure 3** Magnetic resonance imaging and fetopathology of vermian hypoplasia (Case 1). (a) Midline T2-weighted sagittal slice showing normal fourth ventricle, normal posterior/anterior lobe ratio, enlarged fluid space of the posterior fossa and decreased vermian biometry, suggestive of vermian hypoplasia. (b) Fetopathological examination; midline macroscopic view of the vermis, confirming vermian hypoplasia. The vermis is complete but too small and does not cover the cerebellar hemispheres, which is abnormal. Vermian hypoplasia was associated with less pronounced cerebellar hemispheric hypoplasia.

< 5th percentile for gestational age (in the case of disagreement between TCD and weight, weight was used). Destructive lesion was diagnosed if there was evidence of acquired necrotic hemorrhagic damage. Dysplasia was used to define cases of disorganized development, such as abnormal folial pattern or presence of heterotopic nodules of gray matter<sup>2</sup>.

## RESULTS

Twenty-five fetuses were included in this study and our findings regarding the posterior fossa on MRI

and fetopathological examination are summarized in Table 2. The earliest ultrasound examination that raised a suspicion of posterior fossa abnormality was performed at 20 weeks' gestation, and the latest was at 33 + 1 weeks' gestation. In two cases (Cases 9 and 25) the TCD could not be measured sonographically for technical reasons; in the remaining 23 cases, it was normal in 13 fetuses and decreased in 10 fetuses. An enlarged cisterna magna was observed in four cases (Cases 6, 12, 13 and 17).

MRI was performed at a mean gestational age of 31 weeks and fetopathology at a mean gestational age of 33 weeks. The mean interval between MRI and fetopathology was 2 (range, 0–4) weeks. Table 3 shows the degree of agreement between MRI and fetopathological findings with respect to vermian hypoplasia (Figure 3), partial vermian agenesis (Figure 2), cerebellar hemisphere hypoplasia, brain stem hypoplasia (Figure 1) and destructive lesions (Figure 4).

In this series, no complete vermian agenesis was observed. Posterior fossa malformation was never isolated. Associated cerebral or extracerebral abnormalities were detected by ultrasound and MRI or discovered at fetopathological examination. Ventriculomegaly was observed in eight cases and midline abnormalities (mainly corpus callosum abnormalities) in 13 cases. Extracerebral associated abnormalities were numerous and all organs could be involved. Three posterior fossa malformations were part of a syndrome (Fryns, EEC (ectrodactyly, ectodermal dysplasia, cleft lip/palate), CHARGE association (coloboma, heart defect, atresia choanae, retarded growth and development, genital hypoplasia, ear anomalies/deafness)) and two others were associated with an abnormal karyotype (trisomy 18, Fanconi anemia).

## DISCUSSION

Some recent articles about fetal MRI and the analysis of posterior fossa abnormalities have focused on a practical approach, using MRI to classify abnormalities according to the imaging patterns<sup>16</sup>, or on identifying anatomical landmarks of the posterior fossa, using MRI to classify abnormalities according to their prognosis<sup>10</sup>. In one of these articles<sup>10</sup>, it was stated that an accurate diagnosis remains difficult with fetal MRI due to technical limitations and the thinness of the structures. The purpose of this study was to evaluate the accuracy of fetal MRI in diagnosing posterior fossa malformations by analyzing the degree of agreement between MRI and fetopathological findings.

As we have already mentioned, our purpose was not to evaluate the contribution of ultrasound in this field and a systematic midline sagittal slice was not acquired sonographically. It is obvious that detailed ultrasound examination is essential in the anatomical analysis of the posterior fossa<sup>3</sup>, and that many diagnoses can be suggested with ultrasound alone. Using three-dimensional ultrasound, key elements characterizing most anomalies of the posterior fossa can be demonstrated in fetuses<sup>17</sup>.

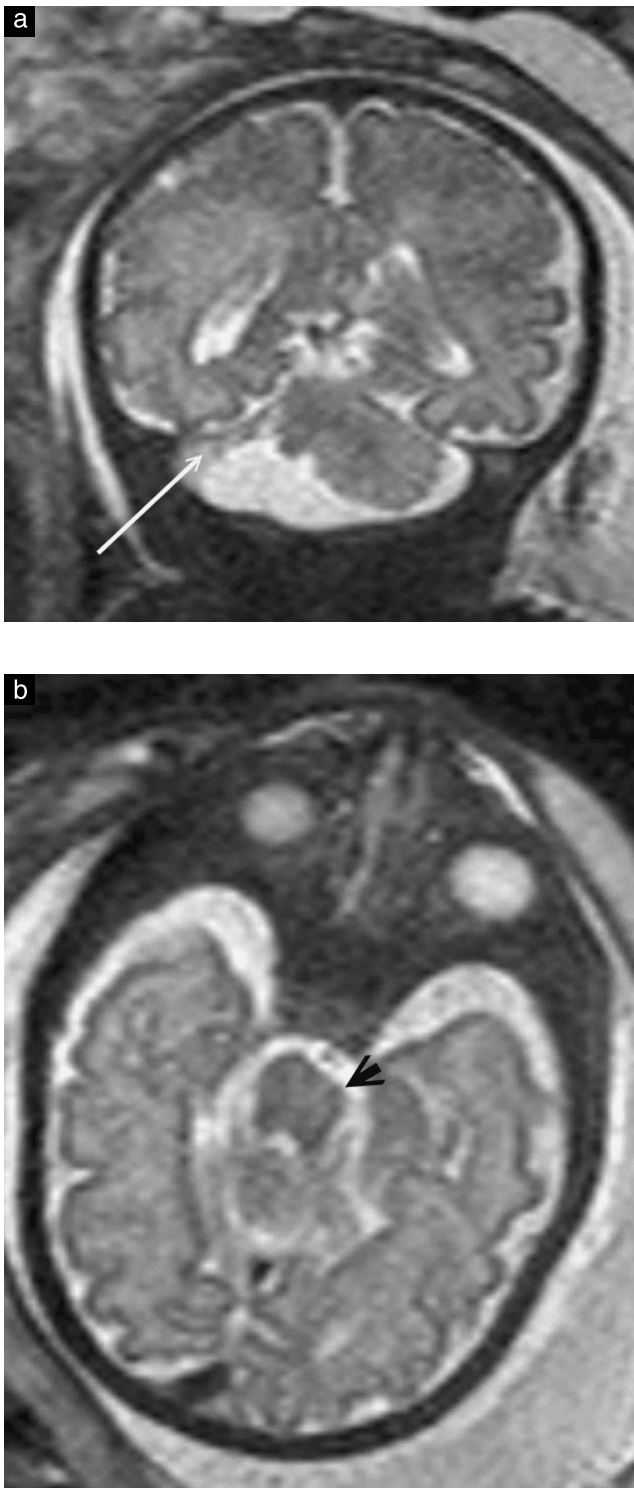


**Figure 4** Magnetic resonance imaging (MRI) and fetopathology of destructive lesion. This patient (Case 25) was referred for MRI at 36 weeks following the detection on ultrasound (performed for breech presentation) of destruction of the right cerebellar hemisphere (the transcerebellar diameter could not be measured). (a) Posterior T2-weighted coronal slice showing the almost complete loss of the right cerebellar hemisphere (arrow). (b) T2-weighted axial slice at the level of the brain stem showing decreased left part of the pons (arrowhead) suggesting Wallerian degeneration. (c) Fetopathological examination; macroscopic view of the cerebellum. The right cerebellar hemisphere is destroyed (arrow). Histological examination showed ischemic–hemorrhagic lesions of both cerebellar hemispheres and confirmed the Wallerian degeneration.

Our study confirms that the measurement of the TCD has an important role in screening practice, but is far from sufficient when the purpose is to define precisely the posterior fossa malformation. The presence of an enlarged cisterna magna (Cases 6, 12, 13 and 17) was not a specific finding and could account for vermian partial agenesis as well as for hypoplasia. Conversely, in this small series, many fetuses with cerebellar hypoplasia or agenesis did not present with an enlarged cisterna magna.

Twelve cases of vermian hypoplasia were observed in our study. There were no false-negative results with MRI but there were four false-positive results. In one case (Case 11), the vermis appeared normally developed, but was flattened caudocranially. There are no published biometric normal values in fetopathology, and in our institution the fetopathological diagnosis of hypoplasia is based on published MRI normal values<sup>8,9</sup> and on a subjective evaluation of the vermis; macroscopic and histological examination are also taken into account. This can account for some disagreement between the methods but it must be stressed that, conversely, there was always good agreement regarding whether the vermis was complete. No case with vermian hypoplasia on MRI was actually vermian partial agenesis.

Regarding vermian partial agenesis (six cases), MRI and fetopathology performed equally well and no false-positive or -negative results were observed. This suggests that even if the spatial resolution of MRI is not sufficient to count the nine lobules of the vermis, a thorough analysis of the biometry and morphology of the vermis and of the fourth ventricle can make it possible to diagnose or eliminate this pathology. However, it must be stressed that this series did not include cases of Dandy–Walker malformation. In fact, during the study period, no termination of pregnancy related to this pathology was performed in our institution. In this disease, the presence of a large posterior fossa cyst and a rotated vermis makes it much more difficult to evaluate the degree of partial vermian agenesis. This

**Table 2** Magnetic resonance imaging (MRI) and fetopathological findings concerning the posterior fossa in 25 fetuses with suspected posterior fossa abnormalities

Case	MRI		Fetopathology		
	GA (weeks) at US*	GA (weeks)	Findings	GA (weeks)	Findings
1	33	34	Global cerebellar hypoplasia	35	Global cerebellar hypoplasia
2	20/24	26	Global cerebellar + pons hypoplasia, very low insertion of tentorium	27	Global cerebellar + pons hypoplasia, very low insertion of tentorium, cerebellar dysplasia (disorganized cortex)
3	23/24	25	Pons + vermian hypoplasia, normal hemispheres	28	Global cerebellar + pons hypoplasia
4	27/27	28	Vermian + hemispheric hypoplasia	29	Vermian hypoplasia with vermian upper displacement by a subvermian cyst
5	33/35	35	Partial vermian agenesis	37	Partial vermian agenesis
6	23/32	32	Global cerebellar + pons hypoplasia	35	Global cerebellar + pons hypoplasia
7	24/29	30	Global cerebellar hypoplasia	33	Global cerebellar hypoplasia
8	30/31	31	Destructive lesions of inferior vermian and cerebellar hemispheres	34	Ischemic-hemorrhagic lesions concerning inferior part of vermian and cerebellar hemispheres
9	22/23	24	Destructive lesions	25	Old ischemic-hemorrhagic lesions involving brain and cerebellum
10	32	33	Pons + vermian hypoplasia	35	Impression of thin pons, but normal weight, normal cerebellum
11	27/31	34	Vermian hypoplasia	34	Complete non-hypoplastic vermian but caudocranial flattening of vermian
12	21	24	Partial vermian agenesis + cerebellar hemisphere hypoplasia	26	Partial vermian agenesis + cerebellar hemisphere hypoplasia
13	35	36	Vermian + hemispheric (mostly left) hypoplasia	38	Vermian + hemispheric (mostly left) hypoplasia
14	23/29	32	Cerebellar + pons hypoplasia	35	Pons hypoplasia + destructive lesions of cerebellar hemispheres, dysplastic cerebellum (cerebellar heterotopias and dysplastic flocculus)
15	32	33	Vermian hypoplasia	34	Normal vermian
16	36	36	Global cerebellar hypoplasia + pons hypoplasia	37	Global asymmetric cerebellar + pons hypoplasia, vermian dysplasia (vermian heterotopias)
17	31	32	Vermian hypoplasia	36	Vermian hypoplasia, vermian dysplasia (vermian heterotopias)
18	29/29	30	Vermian + pons hypoplasia	32	Vermian + pons hypoplasia
19	24/28	31	Partial vermian agenesis + cerebellar hemisphere hypoplasia	34	Partial vermian agenesis + cerebellar hemisphere hypoplasia, vermian dysplasia (vermian heterotopias)
20	22/31	32	Partial vermian agenesis	36	Partial vermian agenesis + vermian dysplasia (vermian heterotopias)
21	22/31	32	Vermian hypoplasia	33	Vermian hypoplasia
22	24/33	33	Partial vermian agenesis + cerebellar hemisphere hypoplasia	35	Partial vermian agenesis + cerebellar hemispheric hypoplasia
23	22/23	24	Partial vermian agenesis	25	Partial vermian agenesis + fourth ventricle cyst
24	26	27	Global cerebellar + pons hypoplasia	27	Global cerebellar + pons hypoplasia
25	36	36	Vermian hypoplasia with right cerebellar hemisphere destruction and Wallerian degeneration	36	Ischemic-hemorrhagic lesions of both cerebellar hemispheres and Wallerian degeneration

\*Gestational age (GA) at discovery of the posterior fossa abnormality with ultrasound (US)/GA at which US was performed before MRI.

has consequences for the evaluation of the outcome according to Klein *et al.*<sup>18</sup>. Partial vermian agenesis must be differentiated from normal but incompletely rotated vermian. Rotation of the vermian is usually completed at 17.5 weeks<sup>19</sup>, but even later incomplete rotation may be observed. The diagnosis is based on normal vermian size and morphology and preserved posterior/anterior lobe ratio<sup>20</sup>.

Regarding cerebellar hemisphere hypoplasia, the comparison of MRI and fetopathology showed two false-positive results (Cases 4 and 14) and one false-negative result (Case 3). In one case (Case 14), the fetopathological examination found small foci of necrosis and hemorrhage that were not seen with MRI and led to the diagnosis of destructive lesion. The other false-negative or false-positive cases could be explained by the fact that weight

**Table 3** Comparison of magnetic resonance imaging (MRI) and fetopathological findings in 25 fetuses with suspected posterior fossa abnormalities, with respect to vermian hypoplasia, partial vermian agenesis, cerebellar hemisphere hypoplasia, brain stem hypoplasia, destructive lesions

MRI	Fetopathology	
	+ve finding (n)	-ve finding (n)
Vermian hypoplasia		
+ve finding	12	4
-ve finding	0	9
Partial vermian agenesis		
+ve finding	6	0
-ve finding	0	19
Cerebellar hemisphere hypoplasia		
+ve finding	10	2
-ve finding	1	12
Brain stem hypoplasia		
+ve finding	7	1
-ve finding	0	17
Destructive lesions		
+ve finding	3	0
-ve finding	1	21

+ve, positive; -ve, negative.

had more value than had TCD in our fetopathological definition of cerebellar hemisphere hypoplasia.

Seven fetuses presented brain stem hypoplasia. There was very good agreement between both methods, as only one false-positive result was found (Case 10) and there were no false negatives. The diagnosis of brain stem hypoplasia is partially subjective in both methods, since there are no published biometric standards in MRI, and the brain stem is weighed with the cerebellum in fetopathology. Nevertheless, the absence of the bulge of the pons and/or the appearance of a thin brain stem seem to be reliable findings. However, there is undoubtedly a necessity to refine both methods.

There was also very good agreement regarding destructive lesions. Three out of four cases were diagnosed by MRI. One was overlooked and this case has already been discussed above (Case 14). Partial or complete loss of anatomical structure, focal decreased biometry with sometimes abnormal signal seem to be reliable findings. Of course, small foci of necrosis or hemorrhage can be overlooked by MRI.

It is noteworthy that in this series, determination of the type of malformation was obtained with T2 sequences only. T1 sequences did not provide additional information and we did not observe cases with T1 signal abnormalities even in the four cases of destructive lesions.

In six cases (Cases 2, 14, 16, 17, 19 and 20), the vermis was considered dysplastic on fetopathology because a disorganized development, such as an abnormal folial pattern mainly at the posterior level, or the presence of heterotopic nodules of gray matter, was observed. These subtle abnormalities can be detected histologically but are usually not responsible for signal abnormalities and are therefore overlooked by fetal MRI. MRI patterns

of abnormal cerebellar foliation have been reported on postnatal examination<sup>21,22</sup>, but the poor spatial resolution of fetal MRI makes this much more difficult to detect in the prenatal period. To our knowledge, only one case has been reported in a fetus, and this appeared as a focal parenchymal hypertrophy<sup>23</sup>.

No rhombencephalosynapsis was observed in our series: this very rare malformation can be detected by ultrasound and MRI<sup>16,24</sup>. The cerebellum appears as a single 'block' with a characteristic transverse folding and significantly reduced TCD.

It is noteworthy that none of the posterior fossa malformations observed in our series was isolated.

In conclusion, with the difficulty in diagnosis of posterior fossa abnormalities and their poor prognosis, it seems essential to develop a systematic approach of analysis of the posterior fossa in ultrasound as well as in MRI. Even if fetopathological examination makes it possible to determine more precisely the type of malformation, the assessment remains somewhat subjective. We have shown that, in most cases, good agreement is observed between MRI and fetopathological results, which emphasizes the necessity of establishing a standard anatomical classification system of fetal posterior fossa abnormalities. Such a system could help in defining homogeneous groups of malformations and in the study of their prognosis. In the future, there will undoubtedly be a necessity to refine both modalities, and notably to establish more biometric data, in order to diagnose these pathologies more accurately and to improve parental counseling.

## ACKNOWLEDGMENTS

We thank Vincent Delezoide for correcting the manuscript.

## REFERENCES

1. Raybaud C, Levrier O, Brunel H, Girard N, Farnarier P. MR imaging of fetal brain malformations. *Childs Nerv Syst* 2003; **19**: 455–470.
2. Patel S, Barkovich AJ. Analysis and classification of cerebellar malformations. *AJNR Am J Neuroradiol* 2002; **23**: 1074–1087.
3. Guibaud L, des Portes V. Plea for an anatomical approach to abnormalities of the posterior fossa in prenatal diagnosis. *Ultrasound Obstet Gynecol* 2006; **27**: 477–481.
4. Garel CDA, Elmaleh-Berges M, Menez F, Fallet-Bianco C, Vuillard E, Luton D, Oury JF, Sebag G. Contribution of fetal MR imaging in the evaluation of cerebral ischemic lesions. *AJNR Am J Neuroradiol* 2004; **25**: 1563–1568.
5. Carroll SGM, Porter H, Abdel-Fattah S, Kyle PM, Soothill PW. Correlation of prenatal ultrasound diagnosis and pathologic findings in fetal brain abnormalities. *Ultrasound Obstet Gynecol* 2000; **16**: 149–153.
6. Limperopoulos C, Robertson RL, Estroff JA, Barnewolt C, Levine D, Bassan H, du Plessis AJ. Diagnosis of inferior vermian hypoplasia by fetal magnetic resonance imaging: potential pitfalls and neurodevelopmental outcome. *Am J Obstet Gynecol* 2006; **194**: 1070–1076.



7. Mahony BS, Callen PW, Filly RA, Hoddick WK. The fetal cisterna magna. *Radiology* 1984; **153**: 773–776.
8. Garel C. Fetal cerebral biometry: normal parenchymal findings and ventricular size. *Eur Radiol* 2005; **15**: 809–813.
9. Garel C. Methodology and results. In *MRI of the Fetal Brain*, Garel C (ed). Springer: Berlin, Heidelberg, New York, 2004; 13–114.
10. Adamsbaum C, Moutard ML, Andre C, Merzoug V, Ferey S, Quere MP, Lewin F, Fallet-Bianco C. MRI of the fetal posterior fossa. *Pediatr Radiol* 2005; **35**: 124–140.
11. Twickler DM, Reichel T, McIntire DD, Magee KP, Ramus RM. Fetal central nervous system ventricle and cisterna magna measurements by magnetic resonance imaging. *Am J Obstet Gynecol* 2002; **187**: 927–931.
12. Brunel H, Girard N, Confort-Gouny S, Viola A, Chaumoitre K, D' Ercole C, Figarella-Branger D, Raybaud C, Cozzone P, Panuel M. Fetal brain injury. *J Neuroradiol* 2004; **31**: 123–137.
13. Guihard-Costa AM, Larroche JC. Differential growth between the fetal brain and its infratentorial part. *Early Hum Dev* 1990; **23**: 27–40.
14. Guihard-Costa AM, Menez F, Delezoide AL. Organ weights in human fetuses after formalin fixation: standards by gestational age and body weight. *Pediatr Dev Pathol* 2002; **5**: 559–578.
15. Guihard-Costa AM, Khung S, Delbecque K, Menez F, Delezoide AL. Biometry of face and brain in fetuses with trisomy 21. *Pediatr Res* 2006; **59**: 33–38.
16. Guibaud L. Practical approach to prenatal posterior fossa abnormalities using MRI. *Pediatr Radiol* 2004; **34**: 700–711.
17. Paladini D, Volpe P. Posterior fossa and vermian morphometry in the characterization of fetal cerebellar abnormalities: a prospective three-dimensional ultrasound study. *Ultrasound Obstet Gynecol* 2006; **27**: 482–489.
18. Klein O, Pierre-Kahn A, Boddaert N, Parisot D, Brunelle F. Dandy-Walker malformation: prenatal diagnosis and prognosis. *Childs Nerv Syst* 2003; **19**: 484–489.
19. Bromley B, Nadel AS, Pauker S, Estroff JA, Benacerraf BR. Closure of the cerebellar vermis: evaluation with second trimester US. *Radiology* 1994; **193**: 761–763.
20. Zalel Y, Seidman DS, Brand N, Lipitz S, Achiron R. The development of the fetal vermis: an in-utero sonographic evaluation. *Ultrasound Obstet Gynecol* 2002; **19**: 136–139.
21. Soto-Ares G, Delmaire C, Deries B, Vallee L, Pruvo JP. Cerebellar cortical dysplasia: MR findings in a complex entity. *AJNR Am J Neuroradiol* 2000; **21**: 1511–1519.
22. Demaerel P. Abnormalities of cerebellar foliation and fissuration: classification, neurogenetics and clinicoradiological correlations. *Neuroradiology* 2002; **44**: 639–646.
23. Guibaud L, Desportes V, Godefroy C, Lorthois N, Pracros JP. Semeiologie IRM ante et post-natale d'une dysplasie cérébelleuse hémisphérique focale isolée associant hypertrophie parenchymateuse focale et verticalisation des sillons (Abstract). *J Radiol* 2005; **86**: 1413.
24. Napolitano M, Righini A, Zirpoli S, Rustico M, Nicolini U, Triulzi F. Prenatal magnetic resonance imaging of rhombencephalosynapsis and associated brain anomalies: report of 3 cases. *J Comput Assist Tomogr* 2004; **28**: 762–765.